

# Magnetic Field Diagnostics in the Low Corona from Microwave Circular Polarization Inversion

C. E. ALISSANDRAKIS

*Section of Astro-Geophysics, Department of Physics, University of Ioannina, Greece*  
*E-mail: calissan@cc.uoi.gr*

## Abstract

The characteristics of the observed polarization of radio waves are determined by the emission mechanism and by the propagation conditions in the corona. In the case of weak coupling between the two electromagnetic wave modes, the polarization changes along the ray path, reflecting the local physical conditions; this results in inversion of the sense of circular polarization when a transverse field region (TFR) is crossed. On the contrary, if the wave coupling is strong, the polarization is fixed and its sense does not change when a TFR is crossed. As a result, Stokes  $V$  maps of active regions do not always correspond to the magnetic polarities shown in photospheric magnetograms. The differences depend on the wavelength, the heliographic position of the region, as well as on the density and the magnetic field of the corona, at about  $0.1 R_{\odot}$  above the photosphere. In this short review I present older and recent observation of polarization inversion and will discuss the diagnostics they provide on the magnetic field.

**Key words:** Sun: radio emission — Sun: magnetic fields — Sun: low corona — Circular polarization

## 1. Introduction

The polarization of the extraordinary (e) and ordinary (o) waves in a magnetized plasma, under the geometrical optics approximation, depends on the electron density,  $N_e$ , the magnitude of the magnetic field,  $B$  and the angle between the magnetic field and the line of sight,  $\vartheta$  (see, e.g., Zheleznyakov, 1970). In the general case, the two waves are elliptically polarized in opposite senses. Under conditions prevailing in the solar corona, the polarization is circular for  $\vartheta$  not too close to  $90^\circ$  (quasi-longitudinal propagation; QL) and linear for  $\vartheta \sim 90^\circ$  (quasi-transverse propagation; QT).

As the physical conditions change along the path of the wave, its polarization changes accordingly. This implies that, when the wave crosses a TF region, the sense of its polarization will change, since the sign of the longitudinal component of the magnetic field changes. This happens as long as the geometrical optics approximation is valid, i.e. for not too low values of  $n_e$  and  $B$ . In a more general sense, the situation is described in terms of wave coupling. When the coupling between the e-mode and o-mode waves is weak their polarization properties change along the ray path, whereas when the geometrical optics approximation breaks down the waves are strongly coupled and their polarization remains fixed, even if a TFR is crossed.

Wave coupling has been studied comprehensively by Cohen (1960; see also Zheleznyakov, 1970; Bandiera, 1982). In the case of QL propagation the coupling becomes strong for extremely low values of the density. Of more interest is the case of QT propagation; the coupling coefficient then is:

$$C = a \frac{\omega^4}{N_e B^3} \left\| \frac{d\vartheta}{ds} \right\| \quad (1)$$

where

$$a = \frac{2 \ln 2}{\pi^2} \frac{m_e^4 c^4}{e^5} \quad (2)$$

and the symbols have their usual meaning.

Taking into consideration the effect of wave coupling, the sense of circular polarization does not necessarily change when the waves cross a TFR. In fact, what happens depends on the value of  $C$  at the point, along the ray path, where the longitudinal component of the magnetic field,  $B_\ell$ , vanishes:

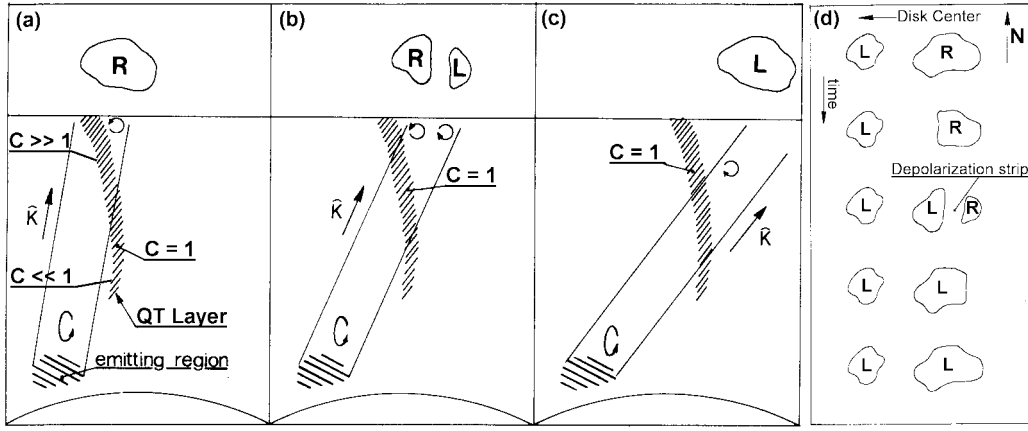


Fig. 1.. Geometry of radiation crossing a region of quasi transverse magnetic field (after Bandiera, 1982)

- If  $C \ll 1$  the polarization changes sense
- If  $C = 1$  the polarization becomes linear (critical coupling)
- If  $C \gg 1$  the sense of polarization does not change

Of particular interest is the case of  $C \approx 1$ , which has been treated by Zheleznyakov and Zlotnik (1963). The resulting polarization is elliptical, with the degree of circular ( $\rho_c$ ) and linear ( $\rho_\ell$ ) polarization given by:

$$\rho_c = -1 + 2 \exp\left(-\frac{\ln 2}{C}\right) \quad (3)$$

$$\rho_\ell = 2 \exp\left(-\frac{\ln 2}{2C}\right) \sqrt{1 - \exp\left(-\frac{\ln 2}{C}\right)} \quad (4)$$

which, for  $C = 1$  give  $\rho_c = 0$  and  $\rho_\ell = 1$ .

We note here that, with continuum receivers used in radio observations, the observation of linearly polarized radiation from the sun is not possible, due to the strong Faraday rotation within the receiver bandwidth. Further difficulties may arise from wave scattering in coronal inhomogeneities (Bastian, 1995). In spite of these difficulties, Alissandrakis and Chiuderi Drago (1994) reported the detection of linearly polarized radiation and measured the Faraday rotation, using a narrow band spectral line receiver.

Consider now a region emitting right circularly polarized radiation, which crosses a TF region on its way to the observer (Figure 1a). When the region is near the disk center, the TFR is crossed higher up in the corona where the density is low and the coupling strong; consequently the observed polarization is the same as the intrinsic. As the region moves towards the West limb (Figure 1b), at a certain point the radiation from the east part of the region will cross the QT layer under conditions of weak coupling and its sense of circular polarization will be inverted. Closer to the limb (Figure 1c), the radiation from the entire emitting region will cross the QT layer under weak coupling conditions and the observer will see left rather than right circular polarization. In the case of an active region, with both left and right circularly polarized components, the *depolarization strip*, i.e. the region of low circular polarization between the two oppositely polarized sources, will be displaced with respect to the photospheric  $B_\ell = 0$  line by an amount which increases as the active region moves towards the limb (Figure 1d). For a region in the Eastern hemisphere the situation is the reverse: near the limb the observed sense of circular polarization will be that of the preceding part. In all cases, it is the limbward side of the active region that may suffer polarization inversion.

An example of relevant observations is shown in Figure 2. Notice that on May 22, near the East limb, the entire region shows left hand circular polarization, while the bipolar structure of the magnetic field is revealed on May 27, after the central meridian crossing.

The position of the depolarization strip depends on wavelength. Equation (1) implies that  $C$  is higher at short wavelengths, which means that the region of critical coupling moves lower in the corona; as a result the depolarization strip is closer to the photospheric  $B_\ell = 0$  line at short wavelengths. The inversion is first observed at long wavelengths and, as the region moves towards the limb, it appears at progressively shorter wavelengths. This is shown in Figure

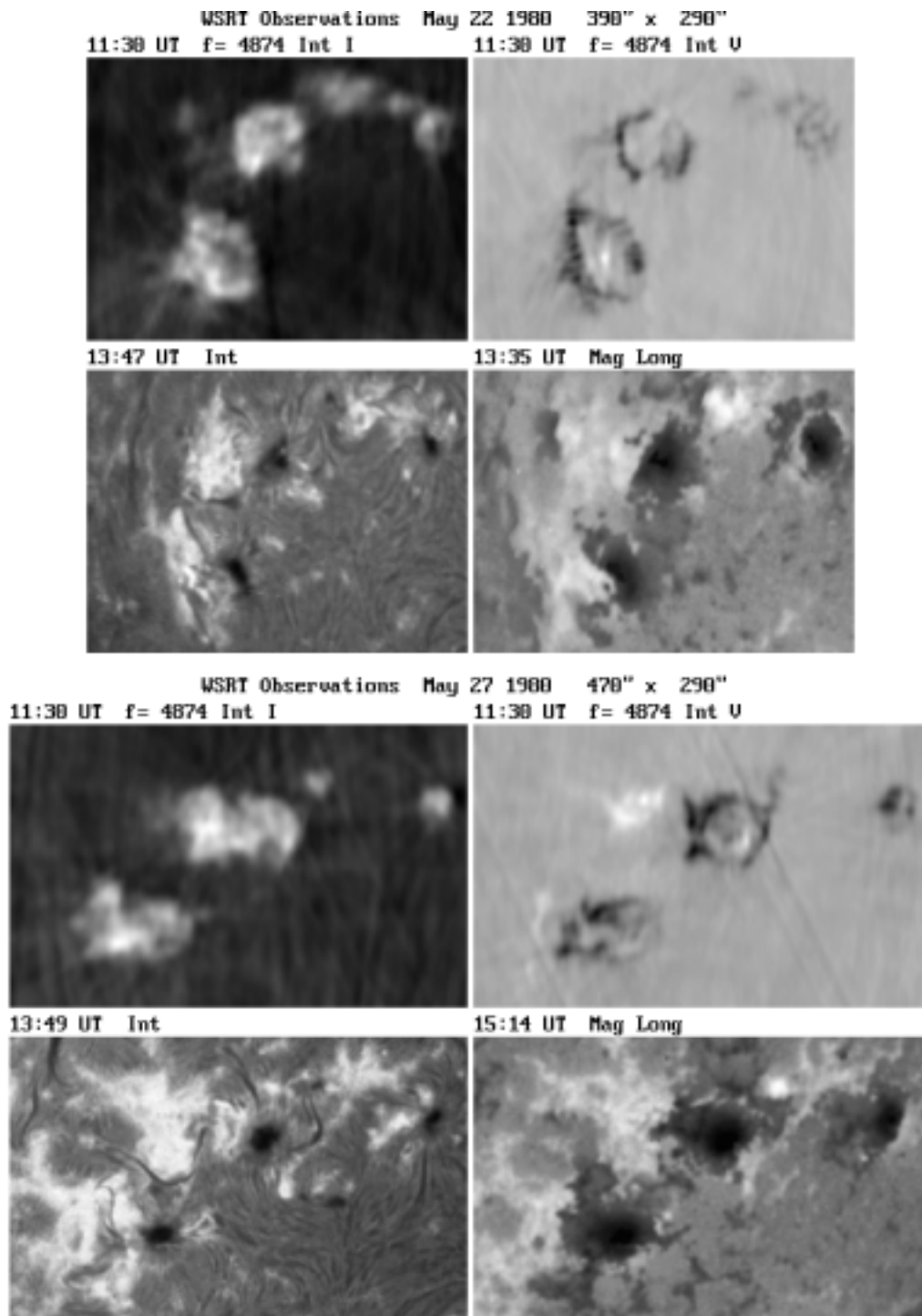


Fig. 2.. WSRT observations of an active region complex, together with  $H\alpha$  photographs and KPNO magnetograms near the East limb (top) and after central meridian crossing (bottom). Right hand circular polarization is white. (Adapted from Kundu and Alissandrakis, 1984)

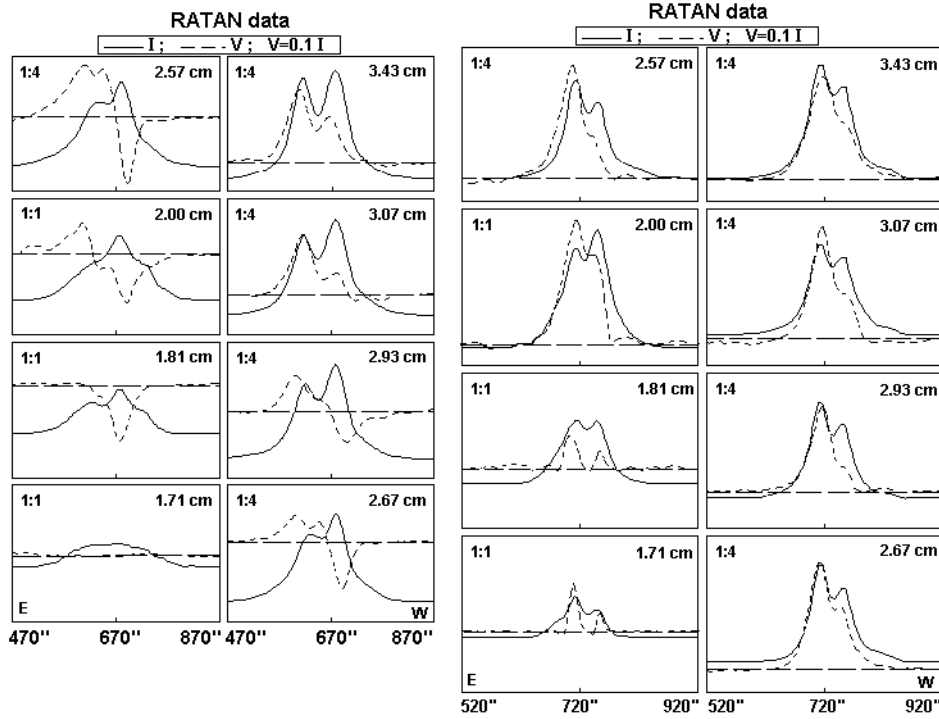


Fig. 3. RATAN-600 multi-frequency Stokes  $I$  and  $V$  data during August 22 and 23, 1992, for an active region approaching the West limb. (From Ryabov et al. 1999)

3, which presents one-dimensional RATAN-600 data at several frequencies over two days. The inversion of the limbward source occurred between 2.93 and 3.07 cm, while on the second day the inversion is seen at wavelengths as short as 1.71 cm.

Notice that the above discussion is independent on the intrinsic polarization of the wave at the site of its generation. Propagation effects, at longer wavelengths in particular, can change considerably the sense of circular polarization expected on the basis of the emission mechanism. The observations give a picture of the magnetic field polarity not at the source of the emission, but the height where  $C = 1$ . Therefore one should be careful in inferring the polarity of the magnetic field on the basis of  $V$  maps. One point made by Kundu and Alissandrakis (1984) is that, due to expected smoother geometry of the coronal magnetic field, small scale magnetic structures should not be detectable on  $V$  maps. Another important point raised by Alissandrakis and Preka-Papadema (1984) concerns the identification of the magnetic polarity of microwave burst footpoints, which should also be affected by propagation effects (see also Alissandrakis et al., 1993).

The crossing of a TRF is not the only known mechanism of polarization inversion. It has been pointed out (e.g. Zheleznyakov et al., 1996) that the geometrical optics approximation is violated and mode coupling occurs also in the case of radiation crossing plasma current sheets.

## 2. Diagnostics

Several methods of diagnostics of the magnetic field exist; the choice depends on the available data. For example, if two or one-dimensional information at a single frequency is available over several days, the distance,  $q$ , of the depolarization strip from the photospheric  $B_\ell = 0$  line can be measured. Using a dipole approximation for the large scale magnetic field of an active region Kundu and Alissandrakis (1984) derived the following expression:

$$q = -2\beta \left( \frac{\alpha - \ell}{3} \right)^{7/8} \quad (5)$$

where  $\alpha$  is the dipole inclination,  $\ell$  the longitude,  $\beta = \frac{N_e d^3}{6a\omega^4}$  and  $d$  is the dipole moment. They determined  $\beta$  and  $\alpha$  by fitting the data, and from those the height of the critical point and the quantity  $N_e d^3$ . Assuming a reasonable

Table 1. Coronal parameters from circular polarization inversion.

Authors	Wavelength (cm)	Height (cm)	Height ( $R_{\odot}$ )	$N_e$ ( $\text{cm}^{-3}$ )	B (G)
Kundu & Alissandrakis (1984)	6.16	$1.1 \times 10^{10}$ $1.3 \times 10^{10}$	0.16 0.19	$10^8$ $10^8$	20 10
Alissandrakis et al. (1996)	6.16	$1. \times 10^{10}$	0.14	$6.4 \times 10^7$	16
Gelfreikh et al. (1987)	2 – 4	$1.2 \times 10^{10}$	0.17	$10^9$	16
Nagelis & Ryabov (1992)	2 – 4	$3.8 \times 10^9$	0.05		26
Lang et al. (1993)	2 – 4	$(0.5 - 2.0) \times 10^9$ $(2 - 3) \times 10^{10}$	0.07 – 0.29 0.29 – 0.43		50 – 15 10 – 5
Ryabov et al. (1999)	1.71 – 3.43 1.71 – 3.43	$(5.7 - 8.7) \times 10^9$ $(3.7 - 6.4) \times 10^9$	0.08 – 0.12 0.05 – 0.09		65 – 20 125 – 30

value of  $N_e$  they got  $d$  and furthermore  $B$ . The exact value of  $N_e$  is not critical because  $B$  is proportional to the cubic root of the assumed value. Their results, together with those of others, are listed in table 1.

Sometimes high resolution data are available for a single day only. In this case one can extrapolate the photospheric magnetic field and find the height at which the projection of the  $B_{\ell} = 0$  line matches the position of the depolarization strip. The height of the region of critical coupling as well as the magnetic field parameters are obtained from the extrapolation and the electron density can be computed from the condition  $C = 1$  (Alissandrakis et al., 1996). This method, however, does not give a very accurate value of  $N_e$  due to its appearance in the third root in the expression.

Data of  $V$  as a function of both the position and the wavelength are readily available thanks to the RATAN-600 radio telescope. The Pulkovo group (e.g. Peterova and Akhmedov, 1973; Gelfreikh et al., 1987; Nagelis and Ryabov, 1992; Lang et al., 1993) have worked extensively with these and some of their results are included in table 1. Note that the RATAN observations extend to short cm- $\lambda$ , which allows one to access lower heights and stronger magnetic fields.

An in-depth analysis of two days of RATAN-600 data was performed recently by Ryabov et al. (1999); they added modelling of the active region emission, which enabled them to derive the variation of magnetic field as a function of height. Their results are shown in Figure 4.

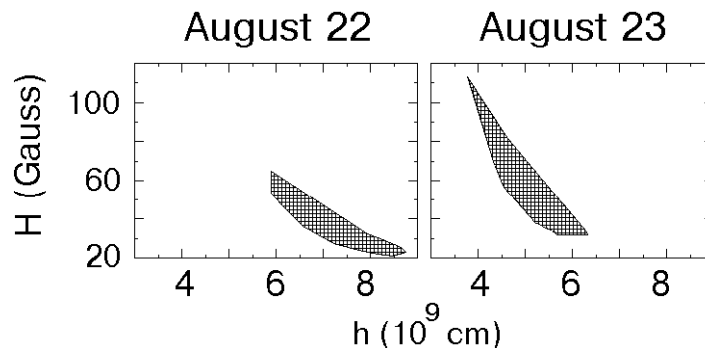


Fig. 4.. The magnetic field as a function of height above an active region, derived from the observations of Figure 3. (From Ryabov et al. 1999)

The diagnostic methods presented so far are based on measurements of the position of the depolarization line in space and/or in frequency. Additional diagnostics can be developed on the basis of the change of the degree of circular polarization as a function of frequency and position, described by equation (3); this expression determines, e.g. the width of the depolarization strip as well as the rate of change of polarization in the direction perpendicular to the strip. The work of Gelfreikh et al. (1997) is in that direction; they used equation (3) to determine the gradient of the magnetic field and obtained typical values in the range of  $10^{-9}$  G/cm at a height of  $1.2 \times 10^{10}$  cm, with a single

value as high as  $2 \times 10^{-5}$  G/cm at a height of  $5 \times 10^9$  cm.

If the intrinsic polarization of the waves were known, one could use equation (3) to obtain a map of the coronal magnetic field in the region where  $C \approx 1$ . Ryabov et al. (1999) using observations from the Nobeyama Radioheliograph, determined the intrinsic polarization on a day without any obvious inversion and subsequently computed the degree of circular polarization for the next day where inversion was observed. In this way they obtained a coronal magnetogram. This appears to be a very powerful method for magnetic field diagnostics, although it is applicable to rather limited regions.

The works presented so far show an almost perfect agreement between observations and theory. However, cases of disagreement have also been reported, mainly in the long decimetric and metric range (Gopalswamy et al., 1991; White et al., 1992). Efforts have been made to interpret these results in terms of current sheets (Gopalswamy et al. 1994) or scattering in inhomogeneities (Bastian, 1995).

### 3. Discussion and Conclusions

The availability of high spatial resolution microwave observations of the sun, as well as the further refinement of the theory of wave propagation and coupling, have provided quantitative information on the magnetic field in a region of the solar atmosphere otherwise inaccessible: the low coronal layers at 0.05 to  $0.4 R_{\odot}$ , which are well above the heights of formation of the radio emission observed in the microwave range. At the same time, the theory of wave propagation gives us a warning not to take at face value the observed circular polarization, as it does not always reflect properties of its source.

The general picture that emerges from these studies is that the magnetic field drops from about 100 G to about 5 Gauss in this height range. A very important advantage of these methods is that they are independent of the emission mechanism. Their primary limitation is that they are applicable only above active regions. With more and better spatial resolution and spectral coverage, we should expect a more complete picture of what the magnetic field looks like above active regions.

This work has been supported in part by a grant from the Greek General Secretariat for Research and Technology and by INTAS grant 94-4625. I would like to thank the Nobeyama 98 LOC for their warm hospitality and financial support.

### References

- Alissandrakis C.E., Borgioli F., Chiuderi Drago F., Hagyard M., Shibasaki K. 1996 *Solar Phys.*, 167, 167  
 Alissandrakis C.E., Chiuderi Drago F. 1994, *ApJL*, 428, L73  
 Alissandrakis C.E., Nindos A., Kundu M.R. 1993, *Solar Phys.*, 147, 343  
 Alissandrakis C.E., Preka-Papadema P. 1984, *A&A*, 139, 507  
 Bandiera R. 1982, *A&A*, 112, 52  
 Bastian T.S. 1995, *Apj*, 439, 494  
 Cohen M.H. 1960, *Apj*, 131, 664  
 Gelfreikh G.B., Peterova N.G., Ryabov B. I. 1987, *Solar Phys.*, 108, 89  
 Gelfreikh G.B., Pilyeva N.A., Ryabov B.I. 1997, *Solar Phys.*, 170, 253  
 Gopalswamy N., White S.M., Kundu M.R. 1991, *ApJ*, 379, 366  
 Gopalswamy N., Zheleznyakov V.V., White S.M., Kundu M.R. 1992, *Solar Phys.*, 155, 339  
 Kundu M.R., Alissandrakis C.E. 1984, *Solar Phys.*, 94, 249  
 Lang K.R. et. al. 1993, *ApJ*, 419, 398  
 Nagelis J., Ryabov B.I 1992, *Kin. Fiz. Neb. Tel*, 8, No 6, 22  
 Peterova N.G., Akhmedov Sh.B. 1973, *Astron. Zh.*, 50, 1220  
 Ryabov B. I., Pilyeva N.A., Alissandrakis C.E., Shibasaki K., Bogod V.M., Garaimov V.I., Gelfreikh G.B. 1999, *Solar Phys.*, in press  
 White S.M., Thejapa G., Kundu M.R. 1992, *Solar Phys.*, 138, 163  
 Zheleznyakov V.V. 1970, *Radio Emission of the Sun and Planets*, Oxford, Pergamon Press  
 Zheleznykov V.V., Zlotnik E.Ya. 1963, *Astron. Zh.*, 40, 633  
 Zheleznykov V.V., Kocharovskiy V.V., Kocharovskiy, V.I.V. 1996, *A&A*, 308, 685